0273-2289/91/3002—0121$02.00

An Effectiveness Factor You Can See

Experimental Visualization of the Effectiveness Factor Concept in a Biological System

CARLES SOLÀ* CARLES CASAS, AND FRANCESC GÒDIA

Unitat d'Enginyeria Química, Universitat Autònoma de Barcelona, Bellaterra 08193, Barcelona, Spain

Received April 3, 1990; Accepted July 12, 1990

ABSTRACT

Effectiveness factor values corresponding to carrageenan immobilized yeast beads packed in a continuous tubular fermenter are obtained from the mathematical modellization of the reactor performing ethanol fermentation. Simultaneously, microscopical direct observation of transversal sections corresponding to two different points in the fermenter is in good agreement with the calculated values: An effectiveness factor near to unity gives a uniform cell distribution in beads, as an effectiveness factor near to 0.75 corresponds to a non-uniform cell growth in beads. This observation gives a visual evidence of the validity of the approach used to treat diffusional limitations in biocatalytic particles.

Index Entries: Effectiveness factor; diffusion and reaction; ethanol fermentation; immobilized cells.

NOMENCLATURE

D_s	effective diffusivity of glucose in carrageenan gel	$cm^2\ min^{-1}$
D_p	effective diffusivity of ethanol in carrageenan gel	$cm^2\ min^{-1}$
K_{ms}	external mass transfer coefficient for glucose	$m\ s^{-1}$

*Author to whom all correspondence and reprint requests should be addressed.

K_{mp}	external mass transfer coefficient for ethanol	m s^{-1}
K'_s	kinetic constant	g L^{-1}
K'_p	kinetic constant	g L^{-1}
P	ethanol concentration	g L^{-1}
P_f	ethanol concentration in the fluid phase	g L^{-1}
P_{sur}	ethanol concentration in the bead surface	g L^{-1}
R	bead radius	mm
S	glucose concentration	g L^{-1}
S_f	glucose concentration in the fluid phase	g L^{-1}
S_{sur}	glucose concentration in the bead surface	g L^{-1}
X	distance from the bead center	mm
X_p	cell concentration in the geal beads	g d.w. L^{-1}
Y_{sp}	fermentation yield	g ethanol/g glucose
υ	specific fermentation rate	h^{-1}
η	effectiveness factor, dimensionless	

INTRODUCTION

The analysis of simultaneous diffusion and reaction inside catalytic particles is one of the most significant examples in chemical engineering of how a problem that in first instance appears to be difficult can be solved, and how an adequate mathematical methodology can help in the comprehension of what is physically happening in the system, thus enabling the prediction of future situations.

From the well-known early works first describing this topic (*1,2*), a very large number of papers and books covering different aspects of such an exciting subject have appeared in the literature (*3–6*), for example, with some really singular contributions in which it is described as a Chemical Engineering Symphony (*7*).

The same methodology has been applied successfully in biochemical engineering, especially with the increasing research interest in that field since 1970, and thereafter, the usefullness of such approach has been demonstrated in the field of immobilized biocatalysts, either using enzymes (*8*) or whole cells (*9*).

In a system with cells immobilized into spherical gel beads, the effect of diffusion is reflected in a concentration gradient inside the particles, thus, the cells are not exposed to the same nutrient concentration and therefore their growth and fermentation rate should be different. The effectiveness factor in a bead is defined as the ratio between the observable actual reaction rate and the reaction rate if the nutrient concentration was uniform in all the beads and equal to that of its surface (in that case, no gradients would be found, and the reaction rate is maximum). Therefore, the presence of nutrient gradients inside the beads will be mathematically

reflected in an effectiveness factor value lower than one (although in some situation with substrate inhibitions, this may cause effectiveness factor values greater than 1). Physically, this situation should cause a nonuniform cell growth inside the particles, as, for example, cells in the center of the bead can easily become nutrient limited, and will not grow.

In this communication, the agreement found between calculation of the effectiveness factor and qualitative microscopical observation of cell growth inside beads is reported. The system in which the experiments were carried out was a tubular packed-bed fermenter with *Saccharomyces cerevisiae* cells immobilized in carrageenan beads, where glucose was continuously fermented to ethanol.

MATERIAL AND METHODS

The characteristics of the immobilized cell fermenter have been previously described (*10*). Basically, it is a tubular packed-bed reactor (2.54 cm internal diameter, 40 cm long) filled with 4% carrageenan gel beads (3.5 mm average diameter) with four sample ports along it. The yeast strain used was identified as *Saccharomyces cerevisiae Hansen*. The fermentation medium contained glucose, yeast extract, and mineral salts. Glucose and ethanol were analyzed by HPLC. To enable the microscopical observation of bead transversal sections, the beads were first fixed with gluteraldehyde, postfixed in OsO_4, dehydrated, and embedded in epoxy resin to obtain solid blocks that could then be cut transversally into 2-μm thick sections using an ultramicrotome. Then, these transversal sections could be observed by phase contrast microscopy. The details of this technique have already been reported (*11*).

RESULTS AND DISCUSSION

The mathematical model describing the reactor performance includes the following aspects.

Intrinsic Fermentation Kinetics

A kinetic model describing the fermentation rate as a function of substrate and product concentrations was obtained from batch experiments using free cell in well-shaked flasks to avoid any mass transfer limitations (*12*). Its equation is

$$\nu = \nu_m \frac{S}{K'_s + S} \cdot \frac{K'_p}{K'_p + P} \qquad (1)$$

where the values of the kinetic parameters for an initial substrate concentration (S_o) of 71 g L^{-1} and 30°C were: $\upsilon_m = 1.8\ h^{-1}$, $K'_s = 1.9$ g L^{-1}, and $K'_p = 7.2$ g L^{-1}.

Flux Model in the Reactor

From residence time distribution experiments made in the reactor during active fermentation, it was determined that deviation from plug flow occurring in the fermenter (mainly resulting from the back-mixing caused by CO_2 produced by fermentation) could be treated using the tanks in series model (*13*). Depending on each flow rate used, the hydrodynamic behavior of the tubular fermenter was equivalent to that of a series of CSTR, from 25 for small flowrate values (approaching plug-flow behavior) to 4 for higher flowrates (maximum back-mixing).

Mass Transfer and Reaction in the Gel Beads

The simultaneous diffusion and reaction inside the immobilized cell particles in steady-state is described by the following differential equations

$$D_s \left(\frac{d^2 S}{d x^2} + \frac{2}{x} \frac{d S}{d x} \right) = \frac{1}{Y_{sp}} \nu (S,P) X_p \qquad (2)$$

$$D_p \left(\frac{d^2 P}{d x^2} + \frac{2}{x} \frac{d P}{d x} \right) = - \nu (S,P) X_p \qquad (3)$$

with the boundary conditions

$$\frac{d S}{d x} = 0 \qquad \text{at} \quad x = 0 \qquad (4)$$

$$D_s \frac{d S}{d x} = k_{ms} (S_f - S_{sur}) \qquad \text{at } x = R \qquad (5)$$

$$\frac{d P}{d x} = 0 \qquad \text{at} \quad x = 0 \qquad (6)$$

$$D_p \frac{d P}{d x} = - k_{mp} (P_{sur} - P_f) \qquad \text{at } x = R \qquad (7)$$

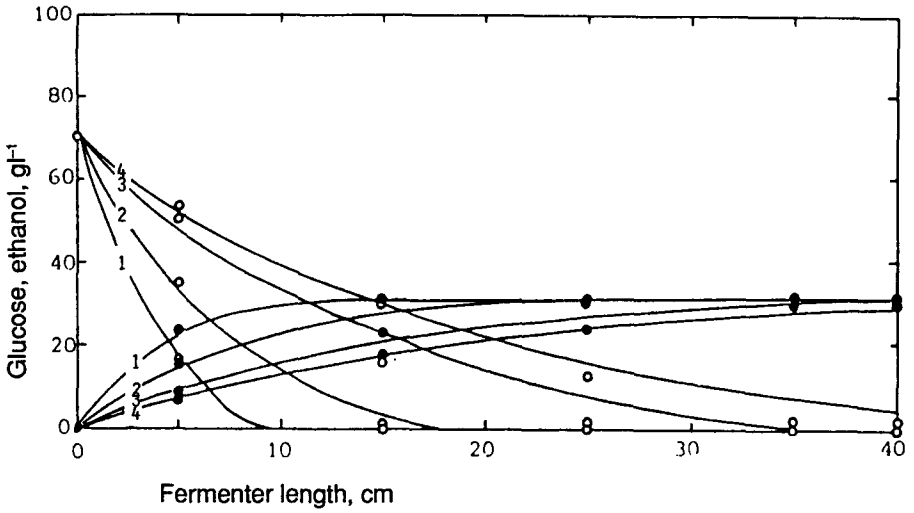

Fig. 1. Results of continuous fermentation modeling for a series of experiments at T=30°C, S_o=71 g L^{-1}, and increasing flowrates of (1) 30, (2) 65, (3) 110, and (4) 155 mL h^{-1}. ○ and ●, experimental glucose and ethanol concentrations, respectively, ——— results of the modelization.

The values for the diffusivity coefficients were taken as those in water, according to the literature (*14*), $D_s = 4\ 10^{-4}$ cm^2 min^{-1}, $D_p = 7.68\ 10^{-1}$ cm^2 min^{-1}. The fermentation rate $v(S,P)$ is given by equation (1). Values for k_{ms} ranged between 5.6–8 10^{-6} m s^{-1}, and k_{mp} between 0.87–1.25 10^{-5} m s^{-1} depending on the liquid flowrate.

The use of this model made possible to describe with reasonable accuracy the steady-state concentration profiles for glucose and ethanol along the packed-bed fermenter at various experimental conditions. In Fig. 1, the results obtained for 71 g L^{-1} initial glucose concentration and 30°C are shown. Symbols correspond to experimental data at various flow rates and solid lines, to the model prediction. Moreover, the effectiveness factor of the biocatalysts beads at any point along the reactor could be calculated by the following equation

$$\eta = \frac{D_s \left.\frac{dS}{dx}\right|_{x=R} \frac{4\pi R^2}{\frac{4}{3}\pi R^3} Y_{sp}}{X_p v_m \frac{S_{sur}}{K'_S + S_{sur}} \frac{K'_P}{K'_P + P_{sur}}} \qquad (8)$$

which, according to the previous definition of effectiveness factor, is the ratio between the actual reaction rate (in steady-state the rate of substrate

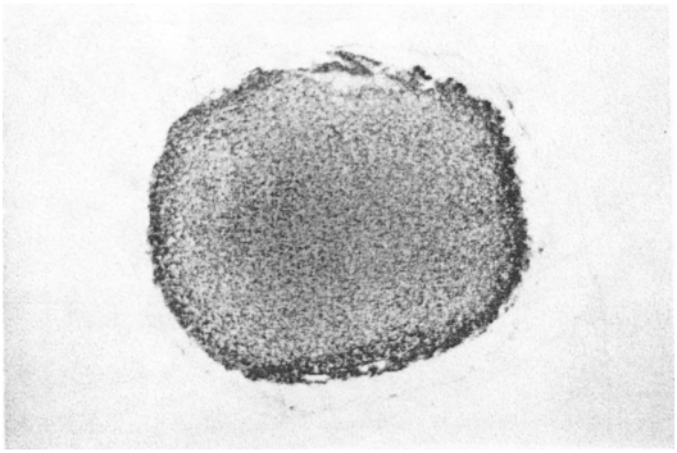

Fig. 2. Microscopical observation of a transversal section of an immobilized cell bead from the fermenter bottom after the experiment in Fig. 1. An external layer with a higher cell density can be clearly observed. The corresponding effectiveness factor value calculated through the model is 0.74.

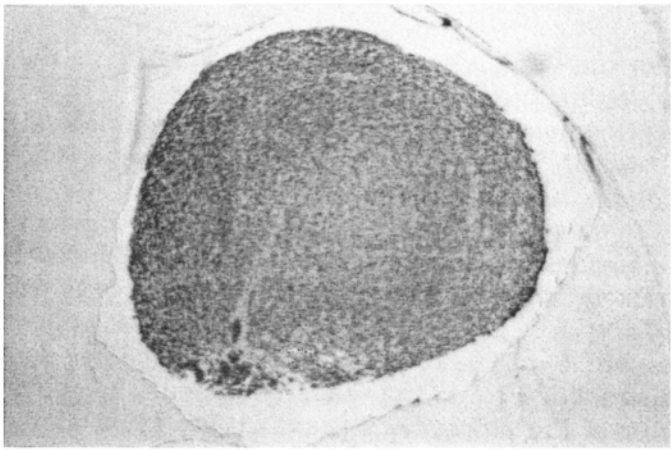

Fig. 3. Microscopical observation of a transversal section of an immobilized cell bead from 20 cm of the fermenter after the experiment in Fig. 1. In this case, a uniform cell distribution can be observed, in agreement with an effectiveness factor calculated through the model of 0.94.

consumption is equal to the rate of substrate transfer from the liquid medium to the particle) and the reaction rate calculated using the concentrations in the surface for the whole particle (that is, in the absence of diffusional limitations). Both can be calculated from the model. The results of η calculation for the experiments already mentioned (Fig. 1) ranged from 0.74 at the bottom section of the fermenter to 0.94 at 15-cm height, remaining constant at this value for the rest of the fermenter.

Furthermore, the microscopical observations of the internal sections corresponding to beads at the bottom of the fermenter and at 20-cm height after the end of the experiment in Fig. 1 are shown in Figs. 2 and 3, respectively. It is interesting to see that in the first case (effectiveness factor 0.74), there is a clear nonuniform distribution of cell density in beads as a consequence of substrate concentration gradients (the grow near the surface was higher because there was more substrate available). However, in Fig. 3, a uniform cell density can be observed, which is in agreement with an $\eta \approx 1$, that is, in the absence of substrate gradients inside the particles.

CONCLUSION

The technique used to obtain transversal sections of immobilized cell beads to be observed microscopically makes it possible to qualitatively see the effect of diffusional limitations in the system. Furthermore, these observations are in agreement with the effectiveness factor calculations made from the mathematical modelization of the fermenter, thus making possible an empirical verification of such approach.

ACKNOWLEDGMENTS

Financial support to this research from the Comisión Asesora de Investigación Cientifica y Técnica, Ministerio de Educación y Ciencia, Spain, is gratefully acknowledged. Thanks are also owing to M. Fca. Roviralta Foundation for providing general laboratory equipment.

REFERENCES

1. Thiele, E. W. (1939), *Ind. Eng. Chem.* **31,** 916–920.
2. Damköhler, G. (1936), *Z. Elektrochem.* **42,** 846–862.
3. Hougen, O. A. (1961), *Ind. Eng. Chem.* **53,** 509–528.
4. Satterfield, C. N. and Sherwood, T. K. (1963), *The Role of Diffusion in Catalysis,* Addison-Wesley, Reading, MA.
5. Thomas, J. M. and Thomas, W. J. (1967), *Introduction to the Principles of Heterogeneous Catalysis,* Academic, NY.
6. Aris, R. (1975), *The Mathematical Theory of Diffusion and Reaction in Permeable Catalysts,* Clarendon, Oxford, UK.
7. Aris, R. (1974), *Chem. Eng. Ed.* **8**(4), 20–40.
8. Engasser, J. M. and Horvath, C. (1976), in *Applied Biochemistry and Bioengineering,* vol. 1 (Wingard, Jr., L. B. and Katchalski-Katzir, E., eds.) pp. 128–220.
9. Karel, S. F., Libicki, S. B., and Roberston, C. R. (1985), *Chem. Eng. Sci.* **40,** 1321–1354.
10. Gòdia, F., Casas, C., and Solà, C. (1987), *Biotechnol. Bioeng.* **30,** 836–843.

11. Gòdia, F., Casas, C., and Solà, C. (1987), *Appl. Microbiol. Biotechnol.* **26,** 342–346.
12. Gòdia, F., Casas, C., and Solà, C. (1988), *J. Chem. Technol. Biotechnol.* **41,** 155–165.
13. Levenspiel, O. (1979), *The Chemical Reactor Omnibook,* OSU Book Stores Inc., Corvallis, OR.
14. Scott, C. D., Woodward, C. A., and Thompson, J. E. (1989), *Enz. Microb. Technol.* **11,** 258–263.